

OPERA

Migration of  
radionuclides in  
Boom Clay  
Annex 2D effects

OPERA-PU-NRG7214

Radioactive substances and ionizing radiation are used in medicine, industry, agriculture, research, education and electricity production. This generates radioactive waste. In the Netherlands, this waste is collected, treated and stored by COVRA (Centrale Organisatie Voor Radioactief Afval). After interim storage for a period of at least 100 years radioactive waste is intended for disposal. There is a world-wide scientific and technical consensus that geological disposal represents the safest long-term option for radioactive waste.

Geological disposal is emplacement of radioactive waste in deep underground formations. The goal of geological disposal is long-term isolation of radioactive waste from our living environment in order to avoid exposure of future generations to ionising radiation from the waste. OPERA (OnderzoeksProgramma Eindberging Radioactief Afval) is the Dutch research programme on geological disposal of radioactive waste.

Within OPERA, researchers of different organisations in different areas of expertise will cooperate on the initial, conditional Safety Cases for the host rocks Boom Clay and Zechstein rock salt. As the radioactive waste disposal process in the Netherlands is at an early, conceptual phase and the previous research programme has ended more than a decade ago, in OPERA a first preliminary or initial safety case will be developed to structure the research necessary for the eventual development of a repository in the Netherlands. The safety case is conditional since only the long-term safety of a generic repository will be assessed. OPERA is financed by the Dutch Ministry of Economic Affairs and the public limited liability company Electriciteits-Produktiemaatschappij Zuid-Nederland (EPZ) and coordinated by COVRA. Further details on OPERA and its outcomes can be accessed at [www.covra.nl](http://www.covra.nl).

This report concerns a study conducted in the framework of OPERA. The conclusions and viewpoints presented in the report are those of the author(s). COVRA may draw modified conclusions, based on additional literature sources and expert opinions. A .pdf version of this document can be downloaded from [www.covra.nl](http://www.covra.nl).

OPERA-PU-NRG7214

Title: Migration of radionuclides in Boom Clay, PA model 'Clay'- Annex 2D effects

Authors: J.C.L. Meeussen, J.B. Grupa,

Date of publication: 11 September 2017

Keywords: migration, Boom Clay, performance analysis

Summary .....	4
Samenvatting.....	4
1. Introduction .....	5
1.1. Background .....	5
1.2. Objectives.....	5
1.3. Realization .....	5
2. Conceptual 2D model for the Boom Clay PA model .....	6
2.1. Geometry .....	6
2.2. Mathematical description.....	8
2.3. Numerical 2D model in Orchestra .....	9
2.4. Analytical solution for the steady state .....	11
2.5. Verification of the steady state concentration profiles .....	16
3. Pseudo 2D model .....	19
3.1. Geometry .....	19
3.2. Test calculations .....	22
3.2.1. Solubility controlled sources.....	22
3.2.2. Unlimited solubility case .....	23
3.3. Evaluation of the pseudo 2D model .....	24
4. Conclusion .....	25
5. References .....	26

## Summary

Theme of the present report is the transport of radionuclides from the repository through the host rock to the aquifer system. The host rock (Boom Clay) is the second model compartment succeeding the source (waste, container and EBS) and is followed by the aquifer system model.

Until now the transport path in the OPAP PA tool has been modelled as one-dimensional. For substances for which migration rates are determined purely by diffusion and linear sorption this is sufficiently accurate. However, for solubility controlled substances, local concentrations are important, which are more accurately calculated by a 2D model. This report compares the 1D approach with a full 2D approach, evaluates the accuracy of this 2D method, and finally introduces an efficient new 1D alternative that approaches the accuracy of the full 2D method in combination with the computational efficiency of the 1D method. This method is called “pseudo” 2D and can be easily included in the 1D PA model for migration of radionuclides in clay.

## Samenvatting

Het onderwerp van dit rapport is het transport van radionucliden vanuit de opbergfaciliteit door het gastgesteente naar het aquifer-systeem. Het gastgesteente (Boomse klei) is het tweede model compartiment na de afvalcontainer/galerijstructuur en wordt gevolgd door het aquifer-systeem model.

Het transport wordt tot dusver gemodelleerd met een 1-dimensionaal model, wat voor puur diffusief transport met lineaire verdeling van stoffen over vaste en opgeloste fase voldoende nauwkeurig is. Voor oplosbaarheidsgecontroleerde nucliden zijn lokale concentraties van belang, en deze zijn nauwkeuriger te berekenen met een 2D-model. In dit rapport wordt de 1D-aanpak vergeleken met een 2D-aanpak. Ten slotte wordt er nog een alternatieve “pseudo 2D” aanpak geïntroduceerd die de nauwkeurigheid van de 2D-aanpak benaderd en deze combineert met de rekenefficiëntie van de 1D-aanpak.

# 1. Introduction

## 1.1. Background

The five-year research programme for the geological disposal of radioactive waste - OPERA - started on 7 July 2011 with an open invitation for research proposals. In these proposals, research was proposed for the tasks described in the OPERA Research Plan (Verhoef & Schröder, Research Plan, 2011).

## 1.2. Objectives

This report describes the execution and results of the research proposed for Task 7.2.1 with the following title in the Research Plan: *PA model for radionuclide migration in Boom Clay*.

The main objective of this task is to set up a PA modelling code for calculating the migration of radionuclides from the waste packages through the Boom Clay host rock to the enclosing geosphere. The proposed modelling and calculation approach is based on the findings of WP 6.1.2 (*Modelling of sorption processes*), WP 6.1.3 (*Modelling of diffusion processes*), WP 6.1.4 (*Mobility and presence of colloidal particles*), WP 4.2 (*Geohydrological boundary conditions for the near-field*), and WP 5.2 (*Properties, evolution and interactions of the Boom Clay*) and served as direct input to Task 7.2.2 (*PA model for radionuclide migration in the rock formation surrounding the host rock*) and Task 7.2.4 (*Integrated modelling environment for safety assessment*).

## 1.3. Realization

This report has been compiled by NRG.

## 2. Conceptual 2D model for the Boom Clay PA model

The PA-model for radionuclide transport in clay as described in OPERA-PU-7212, (Grupa, Meeussen, Rosca-Bocancea, Buhmann, Laggiard, & Wildenborg, 2017) uses the observation that for most nuclides there is, in each clay volume, by approximation a linear relation between the concentration of dissolved radionuclides and the amount of nuclides bound to the clay, i.e. the  $K_d$  approach. If the  $K_d$  approach is valid, it can be shown that for the OPERA disposal concept, the nuclide transport equations in clay reduce to a 1D-diffusion equation.

Although for most nuclides the  $K_d$  approach is adequate, there are a few exceptions. In particular, the concentration of the uranium that leaches from the depleted uranium disposal galleries (see (Verhoef, Neeft, Grupa, & Poley, 2011) is expected to reach the solubility limit for uranium.

The issue was already discussed in (Grupa, Meeussen, Rosca-Bocancea, Buhmann, Laggiard, & Wildenborg, 2017, p. 4.7), where a conservative approach for the steady state solution was suggested.

### 2.1. Geometry

A schematic outline of the OPERA disposal facility (Verhoef, Neeft, Grupa, & Poley, 2011) is given in (Arnold, Vardon, Hicks, Fokkens, & Fokker, 2015). It can be seen that the distance from a disposal gallery to the nearest access shaft (located at the workshop and pilot facility) can vary between roughly 100 m and 2000 m.

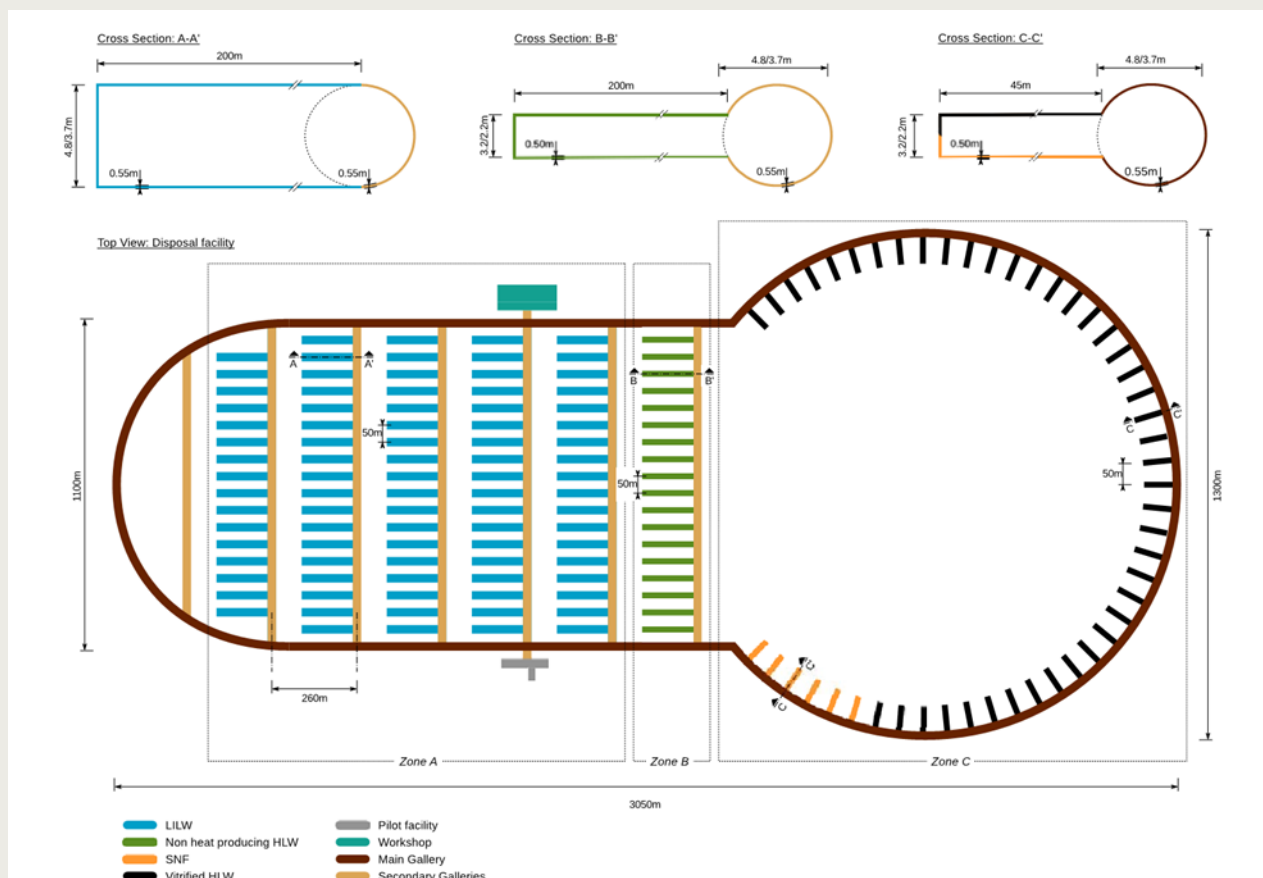


Figure 1 Schematic outline of the OPERA deep geological disposal facility in Boom Clay taken from (Arnold, Vardon, Hicks, Fokkens, & Fokker, 2015)

The LILW section contains amongst others 9060 depleted uranium (DepU) containers, each with a volume of about  $4.6 \text{ m}^3$ . The total volume of the uranium containers is about

40000 m<sup>3</sup>. Since the containers have a cubic shape, there is a large backfill volume in the disposal galleries: about 34000 m<sup>3</sup>.

The diameter of the disposal gallery is about 4 m, so the total length of the disposal tunnels needed to emplace the DepU containers is about 5850 m. The length of each disposal tunnel is about 200 m, including the plug and seal, which is about 15 m long. So the DepU will use about 32 disposal galleries in the LILW section of the OPERA disposal facility.

**Table 1 Summary of the geometry data**

DepU in 9060 Konrad type II containers	40 000 m <sup>3</sup> total volume
EBS backfill	± 34 000 m <sup>3</sup> backfill (foam concrete)
Total volume	± 74 000 m <sup>3</sup>
Disposal tunnel	diameter: 4 m; useable length: 185 m
Tunnel spacing	50 m
Disposal footprint	in total 5800 m tunnel-length in 32 parallel tunnels

Since the waste is disposed in parallel tunnels, the geometry approaches some symmetries that can be used to save numerical calculation work, and to find some analytical solutions. The blue block in Figure 2 is bounded by three areas where the nuclide flux must be zero because of spatial symmetry, and the aquifer, where we assume that the concentration must be much lower than in the clay (for the numerical scheme) or even zero for the analytical solution. At the disposal tunnel boundary, it is assumed that at t=0 the containers fail, and the concentration reaches the solubility limit very quickly (numerical), or reaches the solubility limit instantaneously (analytical).

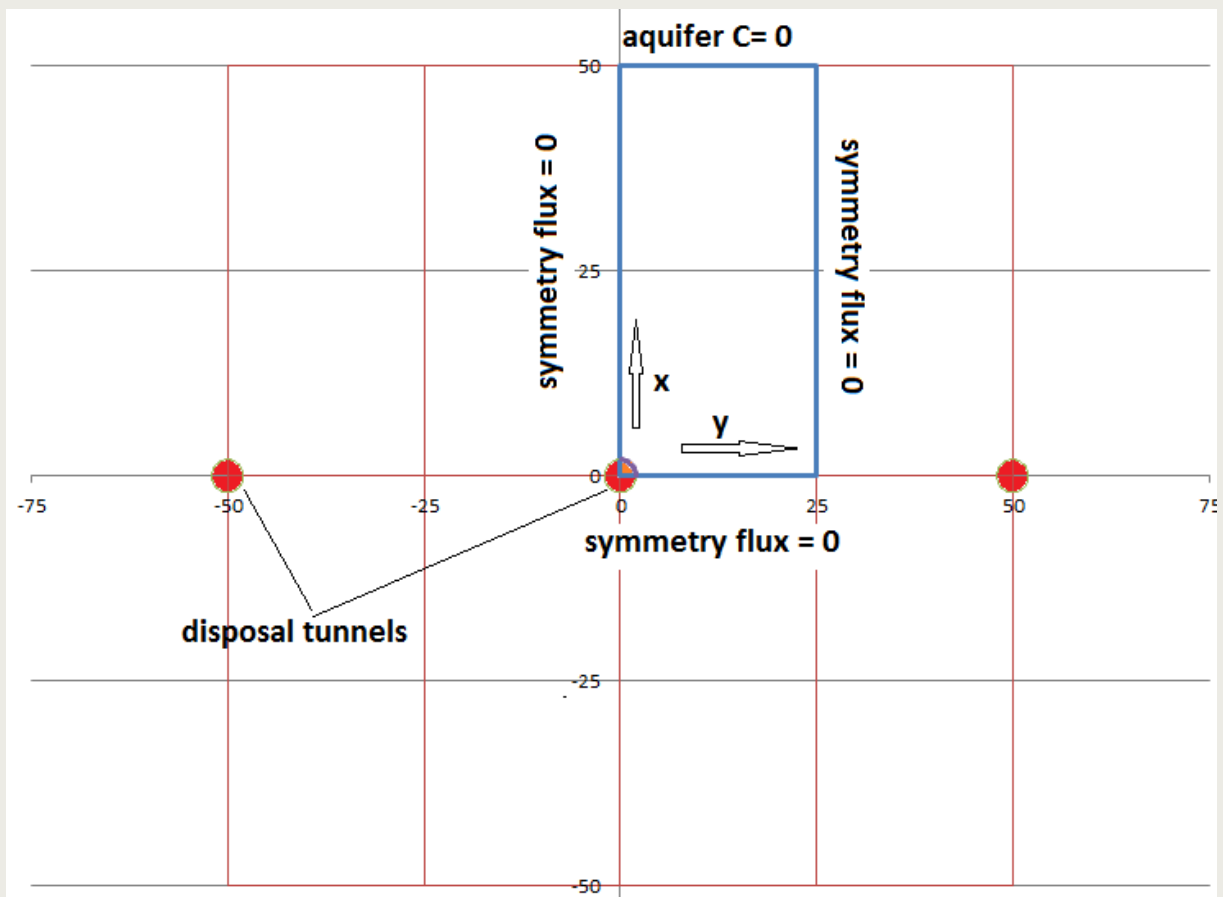


**Figure 2** Symmetries in the disposal geometry

The symmetries are approached at best near the center of the facility, and halfway along the disposal tunnels. At the sides of the system, the volume of undisturbed clay is larger than in the center. Therefore, the migration pathways of nuclides will be longer, and the transport will be slower near the edges of the disposal system.

## 2.2. Mathematical description

For the system under consideration it can be anticipated that the maximum concentration is found at the EBS-clay interface. This concentration can never be higher than the minimum of the solubility limit in the EBS material and the solubility limit in the clay. For all other locations, the concentrations must be below the solubility limits, and can therefore be described by the model described in (Grupa, Meeussen, Rosca-Bocancea, Buhmann, Laggiard, & Wildenborg, 2017).

The mathematical model consist of the following equations, using for the transport (Grupa, Meeussen, Rosca-Bocancea, Buhmann, Laggiard, & Wildenborg, 2017, p. 4.4):

$$J = -\eta_i D_{pore,free} \text{grad}(C_{free}) - \eta_{DOC} D_{pore,DOC} \text{grad}(C_{DOC})$$

and the absorption model (Schröder & Meeussen, 2017, p. 30):

$$n_{absorbed} = K_{d,free} M_s C_{free}$$

$$n_{absorbed} = K_{d,DOC} M_s C_{DOC}$$

where

$J$	diffusive mass flux [mol/m <sup>2</sup> s] of the mobile nuclide
$C_{free}$	aqueous phase concentration of the radionuclides not bound to DOC in the soluble phase [mol/m <sup>3</sup> ],
$D_{pore,free}$	pore diffusion coefficient of aqueous nuclide [m <sup>2</sup> /s],
$\eta_i$	through-diffusion porosity [1] for the species bearing nuclide $i$
$C_{DOC}$	concentration of the radionuclides bound to DOC in the soluble phase [mol/m <sup>3</sup> ],
$D_{pore,DOC}$	pore diffusion coefficient of DOC particles [m <sup>2</sup> /s],
$\eta_{DOC}$	through-diffusion porosity [1] for DOC particles
$n_{adsorbed}$	amount (moles or Bq) of nuclides absorbed to a mass $M$ in the (pore) water
$K_{d,free}$	distribution factor for free ions (m <sup>3</sup> /kg)
$K_{d,DOC}$	distribution factor for nuclides bounded tot DOC (m <sup>3</sup> /kg)
$M_s$	mass of the adsorbing material (kg)

### Solubility limit

Radionuclides originating from the waste can only be transported through the geological formation when they are dissolved in the pore water. Under conditions where the water-solid system is at equilibrium, the maximum concentration of a radionuclide which is soluble in the water depends on the surrounding chemical conditions and is called the 'solubility limit'.

In the model described above two solubility limits can be introduced:  $S_{free}$  and  $S_{DOC}$ , changing the absorption model as follows:

$$C_{free} = \min(S_{free}, \left( \frac{n_{absorbed}}{K_{d,free} M_s} \right))$$



and

$$C_{DOC} = \min(S_{DOC}, \left(\frac{n_{absorbed}}{K_{d,DOC}M_s}\right))$$

The solubility  $S_{free}$  of a given element is the sum of the stoichiometric concentrations of all dissolved species containing the element in equilibrium with a solid phase.

The solubility  $S_{DOC}$  may be determined by the amount of DOC in the aqueous phase, and the absorption capacity of the DOC particles for the radionuclide under consideration.

### 2.3. Numerical 2D model in Orchestra

The PA model for clay as implemented in ORCHESTRA uses a Finite Volume method for calculating the transport and concentrations over time. Finite volume methods use piecewise constant approximation spaces (grid elements). This yields exact conservation statements. The volume integral is converted to a surface integral and the entire physics is specified in terms of fluxes in those surface integrals.

For the 2D implementation in ORCHESTRA, the integral (addressed as the *test function* in the Finite Volume method) is:

$$\begin{aligned} \Delta n_{total} = & A_x \left( (1 - f_{DOC})\eta_i D_{pore,i} + f_{DOC}\eta_{DOC} D_{pore,DOC} \right) \left( \frac{\delta C}{\delta x} \Big|_{x_2} - \frac{\delta C}{\delta x} \Big|_{x_1} \right) \partial t \\ & + A_y \left( (1 - f_{DOC})\eta_i D_{pore,i} + f_{DOC}\eta_{DOC} D_{pore,DOC} \right) \left( \frac{\delta C}{\delta y} \Big|_{y_2} - \frac{\delta C}{\delta y} \Big|_{y_1} \right) \partial t \\ & - \lambda n_{total} \partial t + \sum_p Y_{p,i} \lambda_{p,i} n_{p,i} \partial t \end{aligned}$$

where:

$$C = \frac{n_{total}}{\eta R L_{tunnel} (x_2 - x_1) (y_2 - y_1)}$$

As shown in (Grupa, Meeussen, Rosca-Bocancea, Buhmann, Laggiard, & Wildenborg, 2017, p. 4.4),  $R$  and  $f_{DOC}$  relate with  $K_{d,free}$  and  $K_{d,DOC}$  as follows:

$$\begin{aligned} C &= C_{DOC} + C_{free} \\ R_{DOC} &= 1 + \frac{k_{d,DOC} \rho_{dry}}{\eta} \\ R_{free} &= 1 + \frac{k_{d,free} \rho_{dry}}{\eta} \\ R &= 1 + \frac{(R_{DOC} - 1)(R_{free} - 1)}{R_{DOC} + R_{free} - 2} \\ f_{DOC} &= \frac{\frac{1}{R_{DOC} - 1}}{\frac{1}{R_{DOC} - 1} + \frac{1}{R_{free} - 1}} \end{aligned}$$

ORCHESTRA solves the integral with an Euler explicit scheme.

The equations for  $R$  and  $f_{DOC}$  have been derived under the assumption that concentrations are small, i.e.  $C_{free} < S_{free}$  and  $C_{DOC} < S_{DOC}$ . If  $C_{free} = S_{free}$  or  $C_{DOC} = S_{DOC}$ , the derivation of  $R$  and  $f_{DOC}$  have to be re-evaluated. But this is not part of the present study.

For the present study it is sufficient to assume that there is a solubility limit  $S$  that can be applied to the total concentration  $C$ , as follows:

$$C = C_{DOC} + C_{free} \leq S_{DOC} + S_{free} = S$$

and the values for  $R$  still holds. This is correct if  $f_{DOC} = 0$  or  $f_{DOC} = 1$ .

The OPERA geometry of Figure 2 (25x50 clay segment assuming gallery distance of 50 m and a clay layer thickness of 50m) is modelled as a regular 2d grid of 25 x 50 cells.

There is diffusion between cells, and no flux boundaries at the left, right and bottom. Contact area with waste compartment is at the bottom left. The grid used for the calculation is shown in Figure 3.

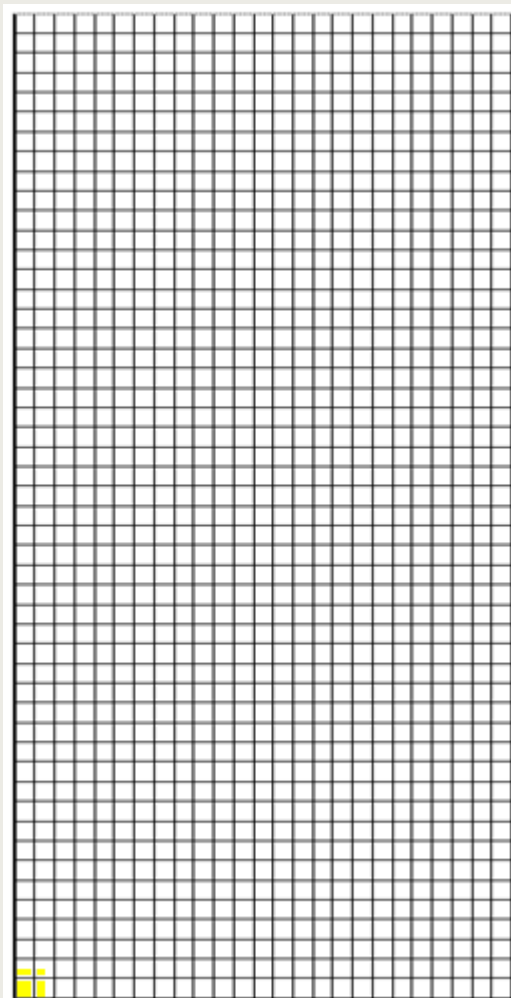


**Figure 3** Calculation grid for the 2D model of the disposal facility and the clay

To verify the model, an analytical steady state concentration profile or solubility limited species has been determined in Section 2.4.

Moreover, the 2D model should give comparable results to the 1D model as described in (Grupa, Meeussen, Rosca-Bocancea, Buhmann, Laggiard, & Wildenborg, 2017) for non-

solubility-limited species such as iodine. The result of the calculation for 1 mol *I-diss* in the source after ca. 40 000 time steps (time = ca. 400 000 years) is shown in Figure 4.

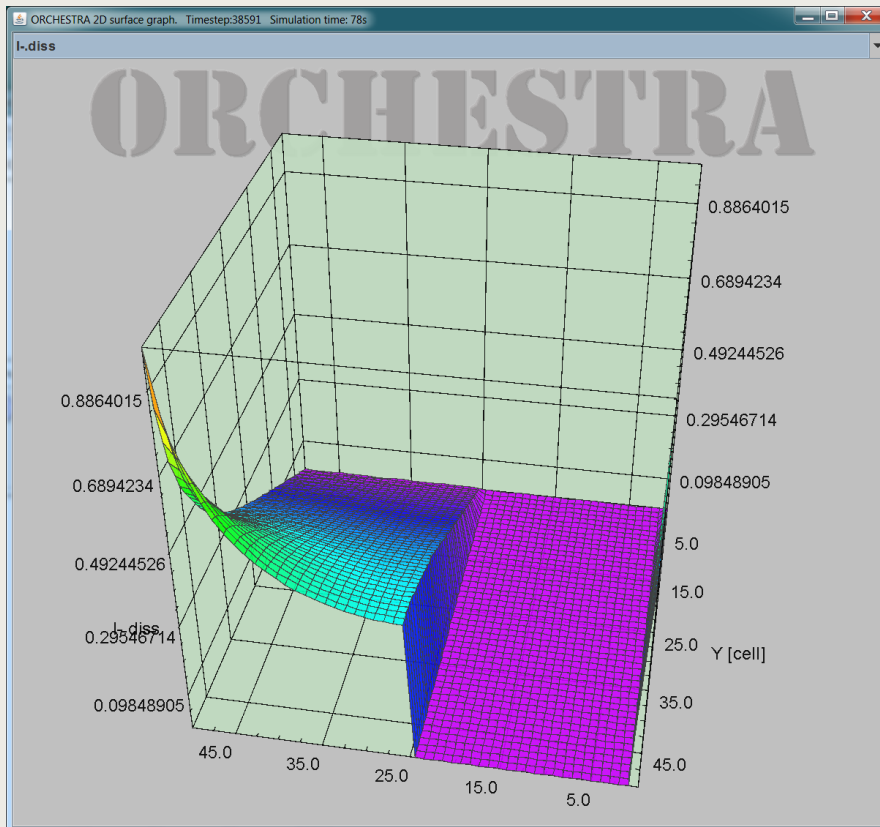


Figure 4 Result of the ORCHESTRA 2D calculation. The grid cells for *y* between zero and 25 m were not used in this calculation.

#### 2.4. Analytical solution for the steady state

In (Grupa, Meeussen, Rosca-Bocancea, Buhmann, Laggiard, & Wildenborg, 2017, p. Annex B) it is shown that the transport equations can be written as:

$$\frac{\partial C}{\partial t} = D_{app} \Delta C$$

and:

$$J = -\eta_0 D_{app} \text{grad}(C)$$

where:

$$D_{app} = \frac{\frac{\eta_{DOC}}{\eta} D_{pore,DOC}}{1 + \frac{K_{d,DOC} \rho_{dry}}{\eta} + \frac{K_{d,DOC}}{K_{d,free}}} + \frac{\frac{\eta_i}{\eta} D_{pore,free}}{1 + \frac{K_{d,free} \rho_{dry}}{\eta} + \frac{K_{d,free}}{K_{d,DOC}}}$$

and:

$$\eta_0 = \frac{(\eta_i D_{pore,free}(1 - f_{DOC}) - \eta_{DOC} D_{pore,DOC} f_{DOC})}{\left( \frac{\frac{\eta_{DOC}}{\eta} D_{pore,DOC}}{1 + \frac{K_{d,DOC} \rho_{dry}}{\eta} + \frac{K_{d,DOC}}{K_{d,free}}} + \frac{\frac{\eta_i}{\eta} D_{pore,free}}{1 + \frac{K_{d,free} \rho_{dry}}{\eta} + \frac{K_{d,free}}{K_{d,DOC}}} \right)}$$

As discussed earlier, the equations for  $D_{app}$  and  $\eta_0$  do not hold if  $C_{free} = S_{free}$  or  $C_{DOC} = S_{DOC}$ . For the purpose of this study it is sufficient to assume that  $f_{DOC} = 0$  or  $f_{DOC} = 1$ , in which case the equations still hold. The treatment of solubility limits for other values of  $f_{DOC}$  is considered in another study (see task 7.4.2).

The solubility limit in the waste EBS compartment or in the clay is mathematically modelled as a Dirichlet boundary condition at the EBS clay interface:

$$C_{\text{EBS-clay-interface}} = S$$

as long as undissolved radionuclide are available in the source.

In the long run, assuming that the amount of radionuclides in the source is sufficiently large, a stationary solution can develop:

$$D_{app} \Delta C = \frac{\partial C}{\partial t} = 0$$

This equation is called the Laplace equation.

- *One gallery in an infinite clay medium*

For the case of on gallery in an infinite clay medium, the geometry is rotation-symmetric, which allows the following solution of the Laplace equation:

$$C(r) = c_1 \ln\left(\frac{r}{r_0}\right) + c_2$$

If  $r_0$  is the location of the EBS-clay interface, the boundary condition is  $C(r_0) = S$ . The stationary solution is that the concentration in the whole infinite clay medium has been raised to  $S$ . The relevance of the above solution shows when two or more galleries are considered, as in the next case.

- *One gallery in a half-infinite clay medium bounded by an aquifer at distance  $L$  from the gallery*

This case can be modelled by the 'source' gallery and a (mathematical) 'sink' gallery opposite to the source gallery. The solution must have the following shape:

$$C(x, y) = c_1 \ln\left(\frac{\sqrt{(x+L)^2 + y^2}}{r_0}\right) + c_2 + c_3 \ln\left(\frac{\sqrt{(x-L)^2 + y^2}}{r_0}\right) + c_4$$

where the single-gallery solution was transformed to Cartesian coordinates with the origin at the aquifer precisely between the two source.

A boundary condition is that  $C \rightarrow 0$  when  $(x, y) \rightarrow \text{infinity}$ , from which we derive that:

$$c_2 + c_4 = 0$$

$$c_3 = -c_1.$$

So:

$$C(x, y) = c_1 \ln \left( \frac{\sqrt{(x + L)^2 + y^2}}{\sqrt{(x - L)^2 + y^2}} \right)$$

If we define the real gallery at  $x = -L$ , then  $c_1 < 0$ .

Note that the steady state concentration profile does not depend on  $D_{app}$  or the porosity. The concentrations are plotted in Figure 5 for  $L = 50$  m and  $c_1 = -1$ .

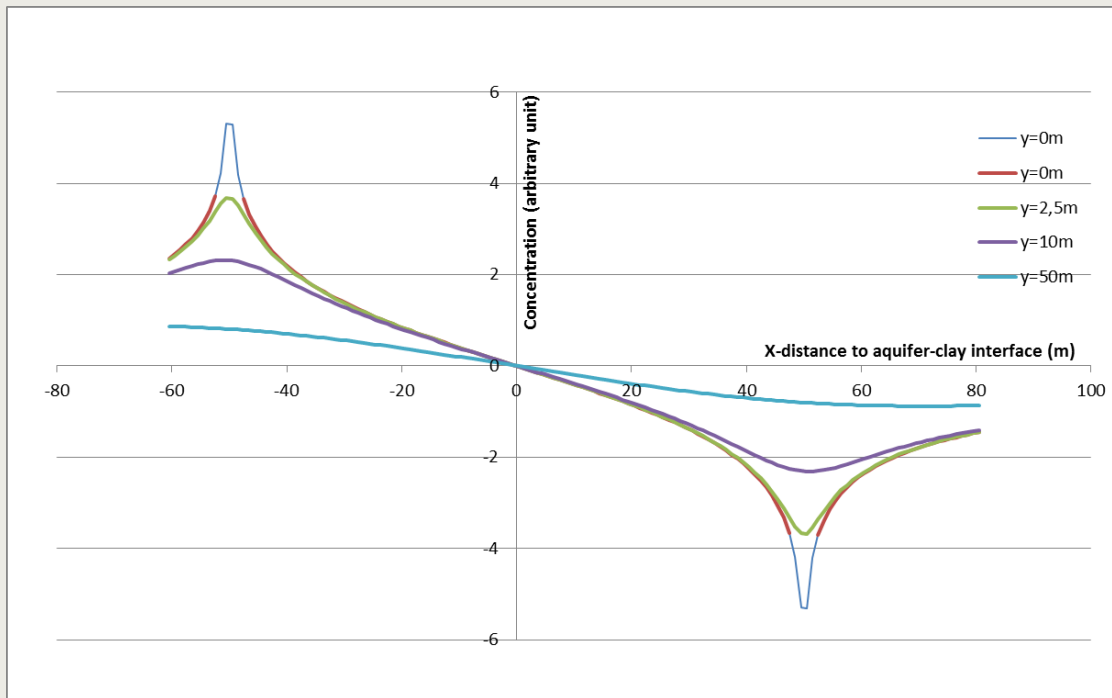


Figure 5 Concentrations for the 'bipolar' system, with a gallery at -50 m in a half infinite clay medium

If we impose a solubility limit  $S=1$  on the EBS-clay interface, for the given radius of the gallery we can determine a value for  $c_1$  such that we find the concentration profile in close approximation. It is not exact, because the iso-concentration lines around each gallery are slightly eccentric because of the influence of the 'sink' gallery at the other side of the aquifer.

radius gallery	0 m	0,5 m	1,5 m	2,5 m	3,5 m	4,5 m
$c_i$ for $S=1$	-1/infinity	-1/5,3	-1/4,2	-1/3,8	-1/3,4	-1/3,0

The flow of radionuclides  $F$  (in Bq/s) into the aquifer can be calculated by integrating the concentration gradients over the clay-aquifer interface defined by  $y = 0$ . The result is:

$$F_{one\ gallery, half\ infinite\ clay\ layer} = \eta_0 D_{app} L_{gallery} \pi (-2c_1)$$

Remarkably, the flow  $F$  does not depend on the distance  $L$  between the gallery and the aquifer for a given value of  $c_1$ . So, if we start a procedure to approximate the

concentration profile in a finite clay layer with thickness  $2L$ , and add as a first step a 'sink' gallery at  $x = -3L$  and a 'source' gallery at  $x = 3L$ , the total flow into the aquifer is zero. If we add another reflection at  $x=\pm 5L$  the flow  $F$  is equal to the 'one gallery' case, add the reflection at  $x=\pm 7L$  and the flow is zero again, and so on.

So, the procedure to model the system of a clay layer between two aquifers will be different to avoid this intermittent behaviour.

- *Parallel galleries in a half-infinite clay medium bounded by an aquifer at distance  $L$  from the gallery*

The flow from  $n$  parallel galleries is additive, so:

$$F_{n \text{ galleries, half infinite clay layer}} = n \eta_0 D_{app} L_{gallery} \pi (-2c_1)$$

The concentration profile for  $n$  galleries at distance  $L_y$  is:

$$C(x, y) = \sum_{i=-(n-1)/2}^{(n-1)/2} c_1 \ln \left( \frac{\sqrt{(x+L)^2 + (y-iL_y)^2}}{\sqrt{(x-L)^2 + (y-iL_y)^2}} \right)$$

- *Parallel galleries in clay layer medium bounded by aquifers at distance  $L$  and  $-L$*

The procedure is to define a base case, and then stepwise add reflections, which should converge to the concentration profile found in a clay layer.

For convenience the origin of the coordinate system is shifted to the center of the clay.

The base case consists of  $n$  source galleries in the center of the clay ( $x=0$ ), ' $n$ ' sink galleries at  $x = 2L$ , each half of the "strength" of the source galleries, and ' $n$ ' sink galleries at  $x = -2L$ :

$$C_{base}(x, y) = \sum_{i=-\frac{n-1}{2}}^{\frac{n-1}{2}} c_1 \ln \left( \frac{\sqrt{(x)^2 + (y-iL_y)^2}}{r_0} \right) +$$

$$- \sum_{i=-\frac{n-1}{2}}^{\frac{n-1}{2}} \frac{c_1}{2} \ln \left( \frac{\sqrt{(x+2L)^2 + (y-iL_y)^2}}{r_0} \right) - \sum_{i=-(n-1)/2}^{(n-1)/2} \frac{c_1}{2} \ln \left( \frac{\sqrt{(x-2L)^2 + (y-iL_y)^2}}{r_0} \right)$$

In the next iteration half a sinks are added at  $x = -2L$  and  $x = 2L$ , and half sources are added at  $x = -4L$  and  $x = 4L$ . Schematically:

base case		- $x = -2L$	++ $x=0$	- $x = 2L$		
1. iteration	+ $x = -4L$	-- $x = -2L$	++ $x=0$	-- $x = 2L$	+ $x=4L$	
- $x = -6L$	++ $x = -4L$	-- $x = -2L$	++ $x=0$	-- $x = 2L$	++ $x=4L$	- $x=6L$

For these geometries the flow to each of the two aquifers is (for each iteration):

$$F_{n \text{ galleries}} = \frac{1}{2} n \eta_0 D_{app} L_{gallery} \pi (-2c_1)$$

For a small number of iterations, the concentration at the location of the aquifers ( $x = L$ ;  $x = -L$ ) is not zero, and the iso-concentration line around the galleries are eccentric. With increasing iterations the concentrations in the aquifers approach zero, and the iso concentration lines approach circles.

- *Results for the OPERA geometry*

Figure 6 shows the concentration profile for the OPERA geometry (for 201 parallel galleries and 10000 reflections), as shown in Figure 2.

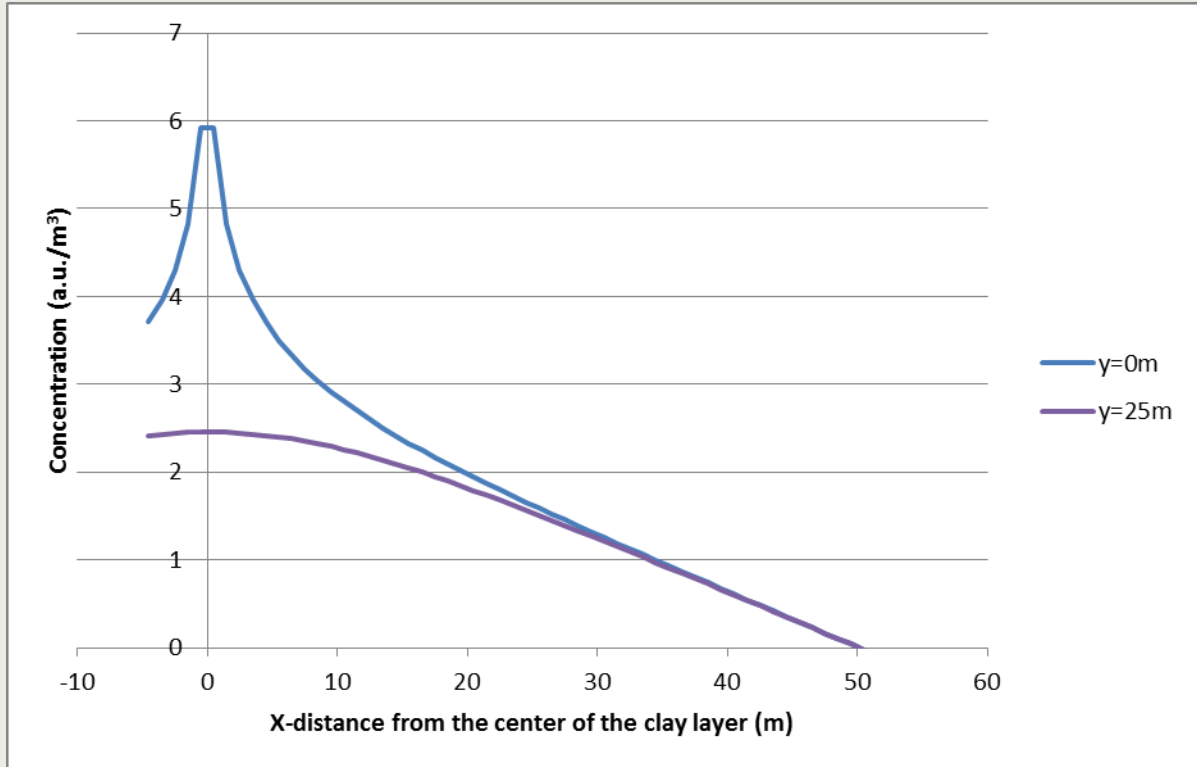


Figure 6 Steady state concentration-profile for the OPERA geometry

The flow  $F_{block}$  (Bq/s) through the area between  $y = 0$  m and  $y = 25$  m, and a length of  $L_{gallery}$  is the total flow from  $n$  galleries divided by  $2n$ :

$$F_{block} = \frac{1}{4} \eta_0 D_{app} L_{gallery} \pi (-2c_1)$$

This allows a consistency check: Figure 6 shows that the concentration gradient into the aquifer (at  $x = 50$ m) is almost constant over  $y$ . So, the flow is:

$$F_{block} = -L_y L_{gallery} \eta_0 D_{app} \frac{dC}{dx}$$

So, using  $c_1 = -1$  and  $L_y = 25$  m:

$$\frac{dC}{dx} = \frac{1}{2} c_1 \pi \frac{1}{L_y} = -0.0628 \left( \frac{\text{a.u.}}{\text{m}^4} \right)$$

From Figure 6 it can be read that  $dC/dx = -0.061 \text{ a.u./m}^4$  at  $x = 50 \text{ m}$

**Table 2 Concentration at various distance from the centre of the gallery for  $c_1 = -1 \text{ au/m}^3$**

rGal (m)	C (au/m <sup>3</sup> )	rGal (m)	C (au/m <sup>3</sup> )	rGal (m)	C (au/m <sup>3</sup> )	rGal (m)	C (au/m <sup>3</sup> )	rGal (m)	C (au/m <sup>3</sup> )
0	Infinity	1	5.225023	2	4.529903	3	4.121153	4	3.82888
0.05	8.221411	1.05	5.176165	2.05	4.505077	3.05	4.104425	4.05	3.816194
0.1	7.528259	1.1	5.129574	2.1	4.480843	3.1	4.087963	4.1	3.803656
0.15	7.122786	1.15	5.085049	2.15	4.457173	3.15	4.071757	4.15	3.791265
0.2	6.835092	1.2	5.042412	2.2	4.43404	3.2	4.055801	4.2	3.779015
0.25	6.611934	1.25	5.001509	2.25	4.411421	3.25	4.040085	4.25	3.766904
0.3	6.429594	1.3	4.962204	2.3	4.389293	3.3	4.024602	4.3	3.754928
0.35	6.275422	1.35	4.924377	2.35	4.367634	3.35	4.009346	4.35	3.743084
0.4	6.141866	1.4	4.887919	2.4	4.346424	3.4	3.99431	4.4	3.731369
0.45	6.024055	1.45	4.852734	2.45	4.325646	3.45	3.979486	4.45	3.71978
0.5	5.918663	1.5	4.818735	2.5	4.305281	3.5	3.96487	4.5	3.708313
0.55	5.823318	1.55	4.785845	2.55	4.285312	3.55	3.950454	4.55	3.696967
0.6	5.736269	1.6	4.753993	2.6	4.265725	3.6	3.936233	4.6	3.685739
0.65	5.656185	1.65	4.723114	2.65	4.246504	3.65	3.922202	4.65	3.674625
0.7	5.582033	1.7	4.693151	2.7	4.227636	3.7	3.908355	4.7	3.663624
0.75	5.512992	1.75	4.66405	2.75	4.209108	3.75	3.894688	4.75	3.652733
0.8	5.448403	1.8	4.635763	2.8	4.190907	3.8	3.881196	4.8	3.641949
0.85	5.387724	1.85	4.608244	2.85	4.173022	3.85	3.867873	4.85	3.631271
0.9	5.330508	1.9	4.581452	2.9	4.155442	3.9	3.854715	4.9	3.620696
0.95	5.27638	1.95	4.55535	2.95	4.138155	3.95	3.841719	4.95	3.610221

Table 2 provides the scaling factors to find the correct value for  $c_1$  for actual nuclide inventory and gallery radius.

As an example: for depleted uranium (DepU), the gallery radius is 2 m, and the solubility limit can be as low as  $1\text{E-}6 \text{ mol/l}$ , so  $c_1 = -2.2\text{E-}10 \text{ mol/m}^3$  (in order to achieve  $1\text{E-}6 \text{ mol/ltr}$  on the EBS-clay interface at 2 m).

The steady state flux into the upper aquifer is, considering the total 5800 m tunnel-length (in 32 parallel tunnels) to emplace all DepU:

$$F_{32 \text{ galleries}}(\text{mol/s}) = \eta_0 D_{app} (\text{m}^2/\text{s}) 4\text{E-}6 (\text{mol/m}^2)$$

### 2.5. Verification of the steady state concentration profiles

In the numerical grid (Figure 3), the size of the modelled EBS-clay interface area is  $3xL_{\text{gal}} \text{ m}^2$  (clay starts at the center point of the second cell, not at the interface between the second and third cell). The gallery radius representing the same size of the EBS-clay interface is 1.95 m. To obtain  $C = 1 \text{ mol/liter}$  at  $r = 1.95\text{m}$ ,  $c_1 = -1/4.56 \text{ mol/liter}$  can be used.



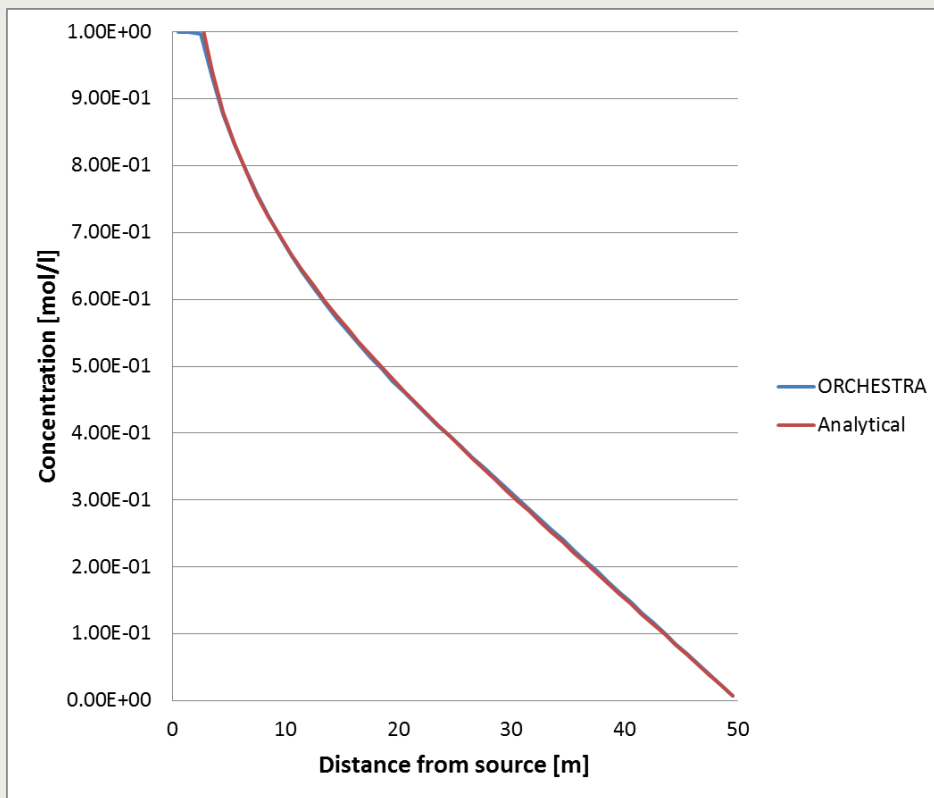


Figure 7 Concentration for varying x at y = 0.5 m (see Figure 2 for the coordinate system)

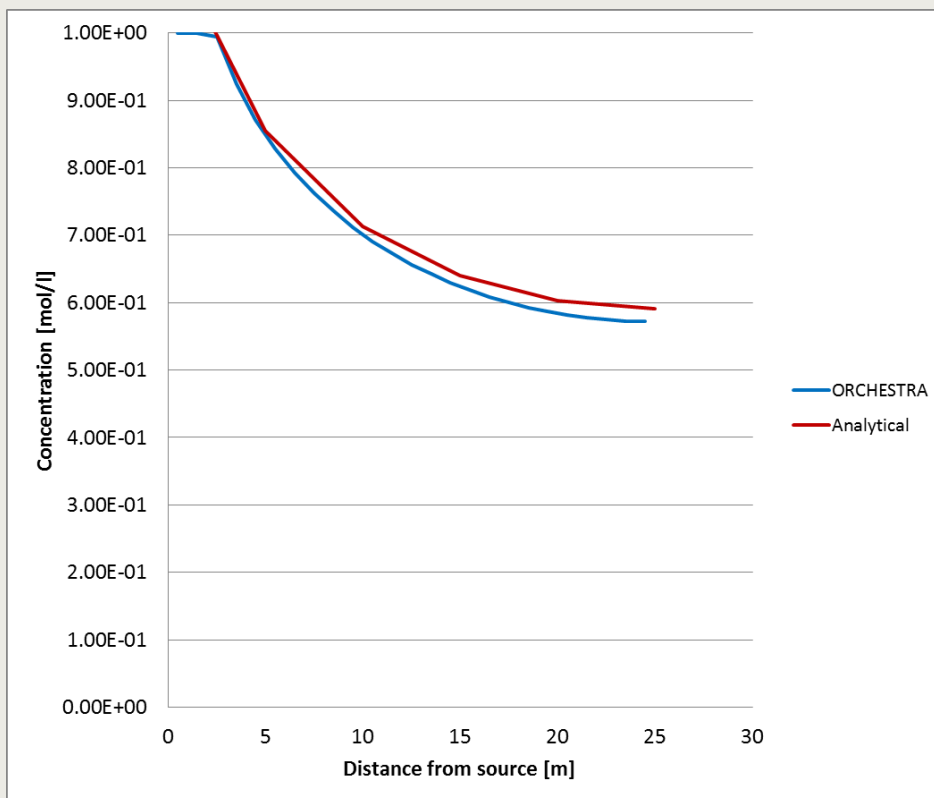


Figure 8 Concentration for varying y at x = 0.5 m (see Figure 2 for the coordinate system)

The steady state flux out of the simulated block is:

$$F_{block} = \frac{1}{4} \eta_0 D_{app} L_{gallery} \pi (-2c_1)$$

For the numerical simulation, the following data were used:

$S = 1$  mol/liter at 2 m from the gallery axis  
 $\eta_0 = 0.3$   
 $D_{app} = 3.156 \times 10^{-3}$  m<sup>2</sup>/year =  $1 \times 10^{-10}$  m<sup>2</sup>/s  
 $L_{gallery} = 1$  m

and for this geometry:

$$c_1 = -1/4.3 \text{ mol/liter} = -1000/4.3 \text{ mol/m}^3$$

Gives:  $F_{block, steady-state} = 0.345$  mol/year

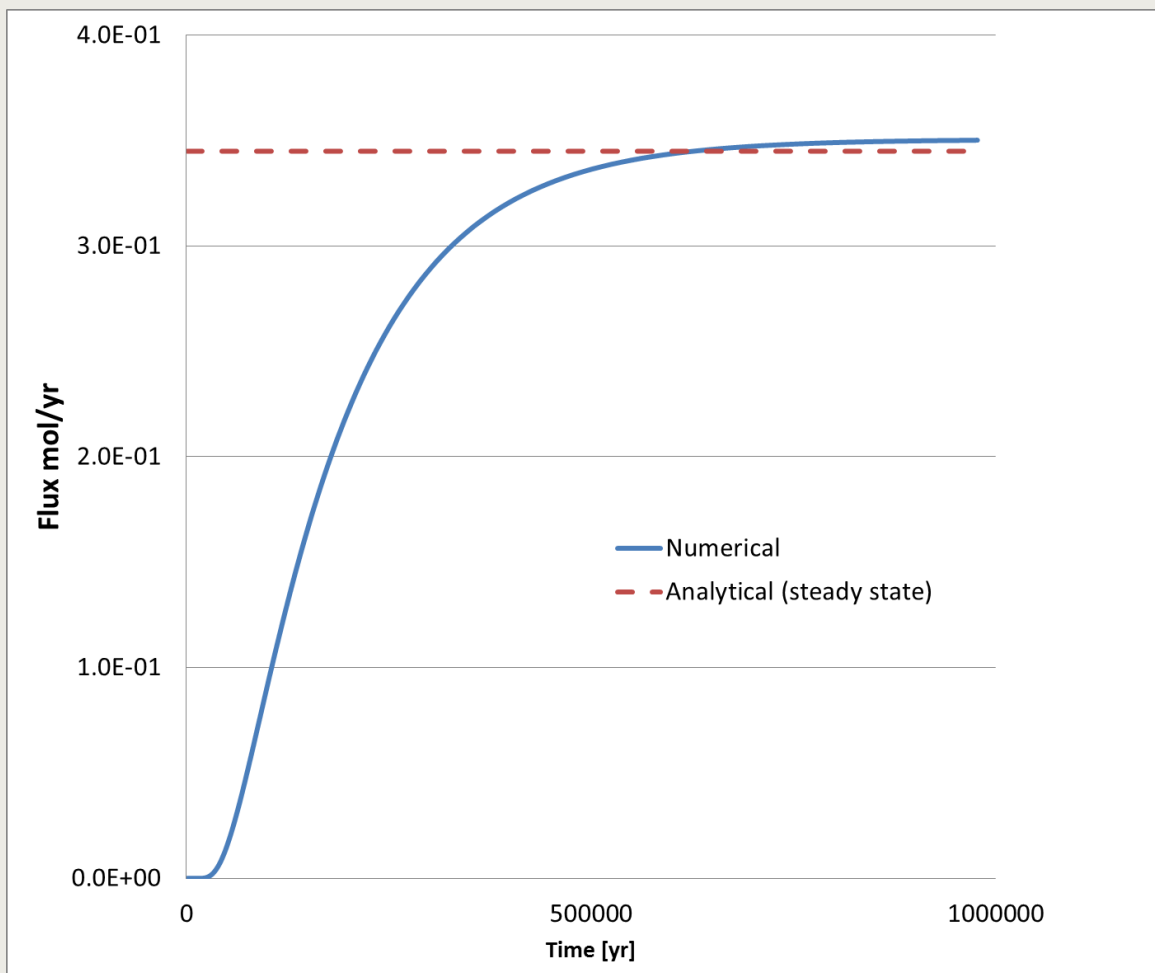


Figure 9 Nuclide flux from the 2D-model block for a solubility limit controlled species

The differences between the analytical and numerical results are relatively small and may be explained by the different shape of the gallery (squared in the numerical model, round in the analytical model) and by the fact that the analytical method has a very slow convergence, so the result may change by a few percent if significantly more iterations are used. This has not been studied further.

## 3. Pseudo 2D model

### 3.1. Geometry

The “pseudo” 2D model presented here is a 1D approximate representation of a 2D grid. The main advantage of the 1D approximation is that it requires much less computational effort. In order to convert the 2D discretization into a 1D version, multiple 2D grid cells have to be merged into single 1D cells. For a good approximation this can best be done by creating single cells in the 1D system that closely follow the iso-concentration lines in the 2D system. Figure 10 shows the lines of equal concentration of the steady state solution. The pseudo 2D model is a good approximation of the concentrations and the fluxes, if the following conditions are fulfilled:

1. the pattern of the iso-concentration lines should not significantly change over time, (basically this will be true in case of fixed system dimensions including those of source and sink)
2. each pseudo-2D numerical cell has a constant concentration in the Y-direction (where the transport is in the X-direction only, see Figure 2 for the definition of the coordinate system), the selected cell widths should be about equidistant.
3. the length of each pseudo 2D cell is corresponding with the 2D-iso-concentration curve starting at the X-coordinate of the pseudo 2D-cell.
4. the concentration gradient between two 2D-iso-concentration curve (representing two adjacent pseudo 2D cells) is constant.

Figure 10 shows that these conditions are fulfilled near the gallery, where the iso-concentration curves are near-circles, and near the aquifer, where the iso-concentration curves are straight.

In the lower right hand corner, the representation is the least accurate. However, because in this area concentration gradients and thus nuclide fluxes are low, the effects on overall fluxes are minimal.

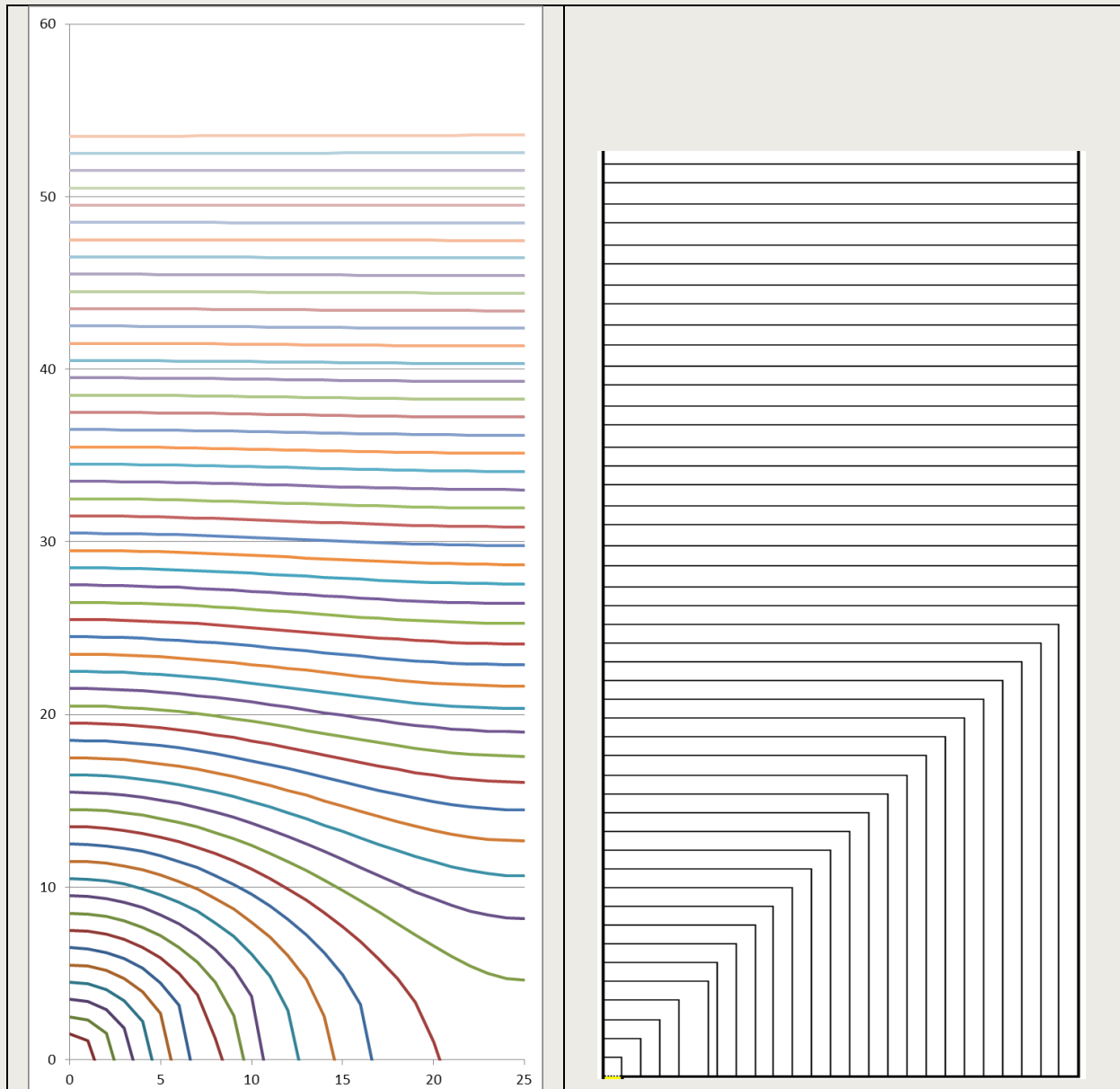


**Figure 10** Iso-concentration lines in the steady state solution (left) - pseudo-2d grid (right)

In the pseudo -2D model the grid was chosen such (see Figure 10 & Table 2) that the summed volume of the pseudo 2D grid elements is equal to the volume of the simulated block of clay. In order to achieve this, the length of the pseudo-2D cells that reach the lower right hand corner has to be exaggerated. This compensates the fact that the distance between the iso-concentration lines in this area is larger than in the other areas.

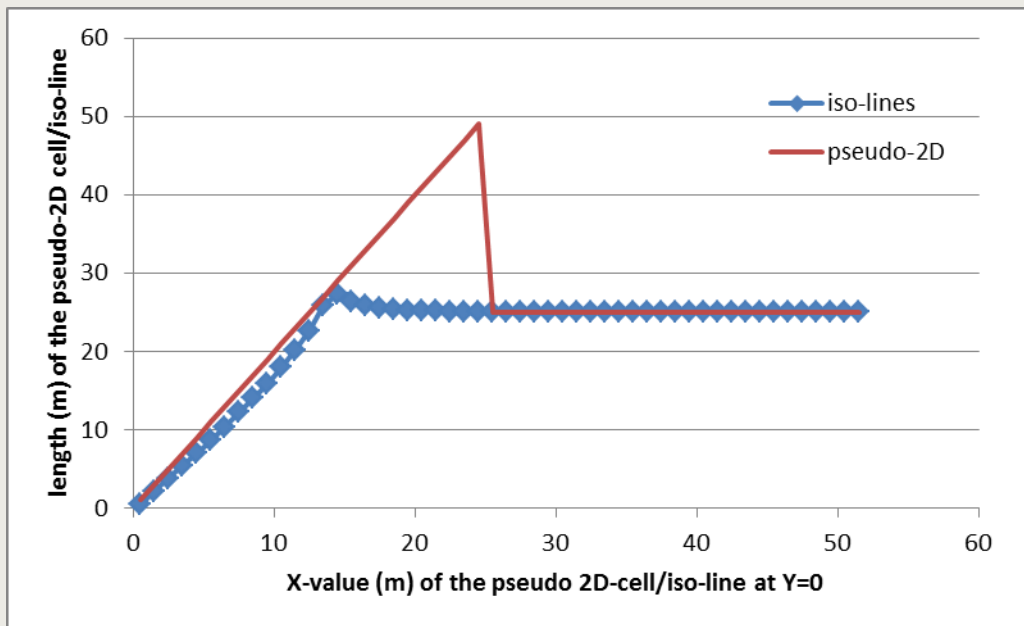


Figure 11 Length of the iso-lines/pseudo-2D cells

In this way, the pseudo-2D grid covers the whole block, accurately models the area around the disposal tunnel (so the concentrations are correct and the impact of a solubility limit is assessed correctly), and also describes the interface between the clay and the aquifer correctly, as this determines the concentration gradients and the out flux into the aquifer.

Table 3 Cell dimensions of the “pseudo” 2D model

Cell dimensions pseudo 2D model				
cellnr	cellvolume [l]	distance to centre[m]	contact area [m2]	
1	1000	0.65	2	
2	3000	0.65	4	
3	5000	0.65	6	
4	7000	0.65	8	
5	9000	0.65	10	
6	11000	0.65	12	
7	13000	0.65	14	
8	15000	0.65	16	
9	17000	0.65	18	
10	19000	0.65	20	
11	21000	0.65	22	
12	23000	0.65	24	
13	25000	0.65	26	
14	27000	0.65	28	
15	29000	0.65	30	
16	31000	0.65	32	
17	33000	0.65	34	
18	35000	0.65	36	
19	37000	0.65	38	
20	39000	0.65	40	
21	41000	0.65	42	
22	43000	0.65	44	
23	45000	0.65	46	

Cell dimensions pseudo 2D model			
cellnr	cellvolume [l]	distance to centre[m]	contact area [m2]
24	47000	0.65	48
25	49000	0.65	50
26	25000	0.5	25
27	25000	0.5	25
28	25000	0.5	25
29	25000	0.5	25
30	25000	0.5	25
31	25000	0.5	25
32	25000	0.5	25
33	25000	0.5	25
34	25000	0.5	25
35	25000	0.5	25
36	25000	0.5	25
37	25000	0.5	25
38	25000	0.5	25
39	25000	0.5	25
40	25000	0.5	25
41	25000	0.5	25
42	25000	0.5	25
43	25000	0.5	25
44	25000	0.5	25
45	25000	0.5	25
46	25000	0.5	25
47	25000	0.5	25
48	25000	0.5	25
49	25000	0.5	25
50	25000	0.5	25
total	1250000	57.5	

### 3.2. Test calculations

Two types of test calculations have been performed. The first type concerns the impact of the 1D, 2D and pseudo-2D grid on the calculation results for solubility limited sources. The second type of test calculations concerns sources where the concentration is not affected by a solubility limit. For test calculations of this second type, the impact of the grid should have no, or minor effects, while for the test calculations of the first type, the grid choice is important.

#### 3.2.1. Solubility controlled sources

Two transient cases were used to compare the 1D, 2D and pseudo 2D model results. The first case assumes a source (a quarter of the waste gallery) with size 1 m, the second case uses a size of 2 m. In both cases the source is assumed to be square. In the 1D model, a grid/cell size of 1 m in the X-direction and 1 m in the Y-direction is used (50 cells), while in the 2D model 25x50 cells of 1x1 m are used. The pseudo 2D model uses 50 cells with size of 1 m in the X-direction and variable size in the Y-direction (see Figure 11).

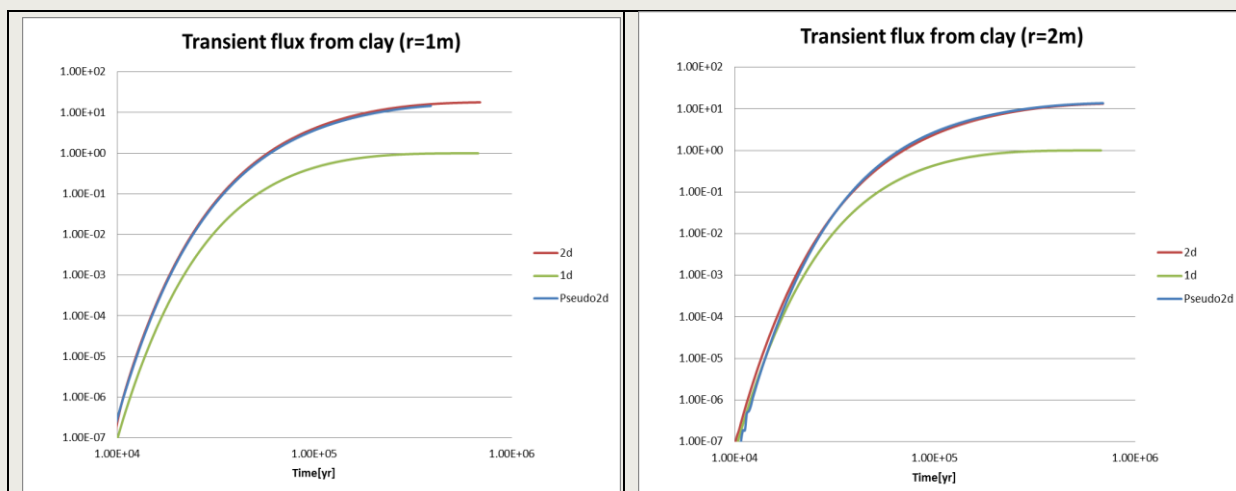


**Figure 12** Calculated relative fluxes for constant (solubility controlled) concentration in source with 1D model, 2D model and “pseudo 2D” model.

From the results shown in Figure 12 it follows that for a fixed concentration system (solubility controlled in the source) the 1D version of the model (in which the width of the grid elements was chosen equal to the gallery diameter 2 m resp. 4 m) significantly underestimates the calculated release fluxes. The fluxes calculated with the 2D version are more than an order of magnitude higher for the 1 m as well as the 2 m radius. As noted in (Grupa, Meeussen, Rosca-Bocancea, Buhmann, Laggiard, & Wildenborg, 2017), the width of the grid elements in the 1D model must be in the range between the gallery diameter (about 4 m) and the gallery spacing (50 m). For the illustration in Figure 12, in retrospective it can be seen that a better choice for the width of the 1D grid elements in the 1D model is 30 m instead of 2 m, and 50 m instead of 4 m.

### 3.2.2. Unlimited solubility case

To confirm that it is correct to use the “pseudo” 2D grid for non-solubility limited nuclides, a test calculation has been performed for a non-solubility limited species, so the concentration in the source will gradually decrease over time because the species diffuse in the clay. The calculated flux from the clay into the aquifer is shown in Figure 13.

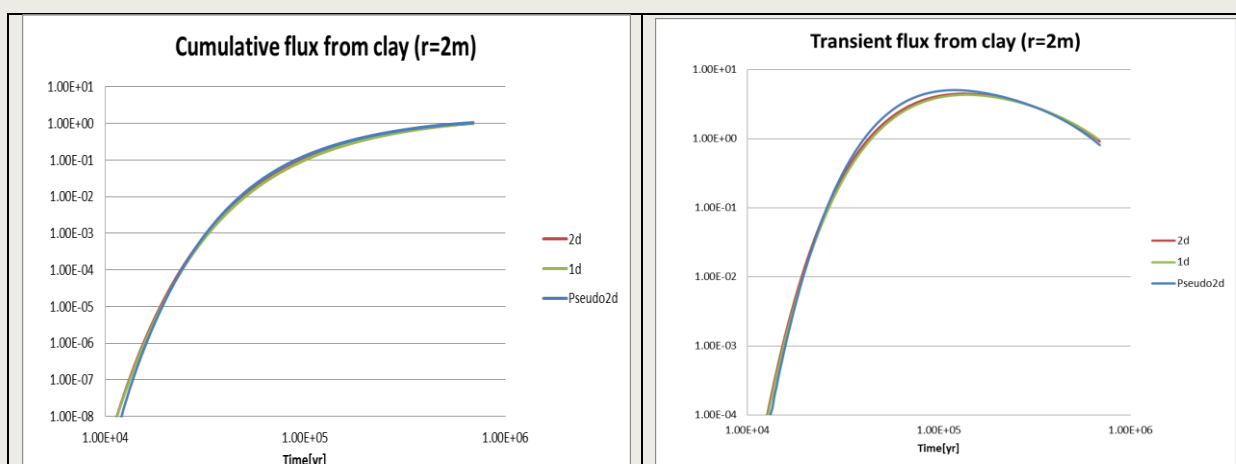


**Figure 13** Calculated relative fluxes for diffusion controlled, variable concentration in source with 1D, 2D and “pseudo 2D model”.

Figure 13 shows that the calculation results for the 1D, 2D and “pseudo” 2D method do not differ significantly for a system in which concentrations in the source are not fixed by a solubility limit, but decrease as a result of diffusion.

These results show that the pseudo-2D model provides a good approximation of the full 2D model for the system dimensions tested here, for diffusion as well as dissolution controlled substances.

### *3.3. Evaluation of the pseudo 2D model*

- In comparison with the 1D model, in the pseudo 2D model there is no need to determine an optimal grid element size, and the concentrations as a function of distance to the gallery are in better agreement with the full 2D model.
- In comparison with the full 2D model, the pseudo 2D model can be much easier implemented in the present PA-tool, the results approach closely the full 2D calculation results, and the calculation uses less computing time.
- The pseudo 2D model models a round gallery, whereas the full 2D grid models a square gallery.
- However, in case other system dimensions are chosen in the future (e.g. depth, gallery diameter, gallery spacing, gallery length, etc.), the pseudo 2D grid has to be adapted and tested against the full 2D model.
- For species that are not affected by a solubility limit, the 1D model (Grupa, Meeussen, Rosca-Bocancea, Buhmann, Laggiard, & Wildenborg, 2017) gives the same result as the 2D and the pseudo 2D models.



## 4. Conclusion

The PA-model for radionuclide transport in clay as described in OPERA-PU-7212, (Grupa, Meeussen, Rosca-Bocancea, Buhmann, Laggiard, & Wildenborg, 2017) uses the observation that the nuclide transport equations in clay reduce to a 1D diffusion equation for most nuclides.

The exception concerns solubility limited nuclides. For example, the concentration of uranium that leaches from the depleted uranium disposal galleries is expected to reach the solubility limit for uranium. In order to deal with a solubility limit, the geometry factor  $g_3$  was introduced in the 1D transport equation (Grupa, Meeussen, Rosca-Bocancea, Buhmann, Laggiard, & Wildenborg, 2017, p. 32), which value has to be determined in specific 2D and 3D calculations.

The pseudo 2D model presented in the previous chapters is a more elaborate approach to the 'geometry factor model', is easy to implement in the PA-model without loss of computing time, and gives a better agreement with full 2D calculations than the 1D model. The implementation of the PA-model has therefore been changed in accordance with the pseudo 2D model.

## 5. References

- Arnold, P., Vardon, P., Hicks, M., Fokkens, J., & Fokker, P. (2015). *A numerical and reliability-based investigation into the technical feasibility of a Dutch radioactive waste repository in Boom Clay*. OPERA-PU-TUD311.
- Grupa, J., Meeussen, J., Rosca-Bocancea, E., Buhmann, D., Laggiard, E., & Wildenborg, A. (2017). *Migration of radionuclides in Boom Clay, PA model 'Clay'*. OPERA-PU-NRG7212.
- Schröder, T., & Meeussen, J. (2017). *Final report on radionuclide sorption in Boom Clay*. OPERA-PU-NRG6123.
- Verhoef, E., & Schröder, T. (2011). *Research Plan*. OPERA-PG-COV004.
- Verhoef, E., Neef, E., Grupa, J., & Poley, A. (2011). *Outline of a disposal concept in clay*. OPERA-PG-COV008 .

## Disclaimer

This report has been prepared at the request and for the sole use of the Client and for the intended purposes as stated in the agreement between the Client and Contractors under which this work was completed.

Contractors have exercised due and customary care in preparing this report, but have not, save as specifically stated, independently verified all information provided by the Client and others. No warranty, expressed or implied is made in relation to the preparation of the report or the contents of this report. Therefore, Contractors are not liable for any damages and/or losses resulting from errors, omissions or misrepresentations of the report.

Any recommendations, opinions and/or findings stated in this report are based on circumstances and facts as received from the Client before the performance of the work by Contractors and/or as they existed at the time Contractors performed the work. Any changes in such circumstances and facts upon which this report is based may adversely affect any recommendations, opinions or findings contained in this report. Contractors have not sought to update the information contained in this report from the time Contractors performed the work.

The Client can only rely on or rights can be derived from the final version of the report; a draft of the report does not bind or obligate Contractors in any way. A third party cannot derive rights from this report and Contractors shall in no event be liable for any use of (the information stated in) this report by third parties.

## **OPERA**

Meer informatie:

Postadres  
Postbus 202  
4380 AE Vlissingen

T 0113-616 666  
F 0113-616 650  
E [info@covra.nl](mailto:info@covra.nl)

[www.covra.nl](http://www.covra.nl)

